Extraction of solid lanoline from raw wool with near-critical ethanol-modified CO_2— A mass transfer model

Abel Valverde*, Francesc Recasens
Department of Chemical Engineering, ETSEIB, UPC, Diagonal 647,
E-08028 Barcelona, Spain
* Corresponding author

Keywords:

Solid-to-fluid, mass-transfer, near-critical CO_2, lanoline solubility.

Abstract:

This study deals with the modelling of the extraction of solid lanoline from raw wool under near-critical conditions using 5% ethanol in CO_2, using our previous experimental data. A mass-transfer model is developed to explain the extraction results at T = 30ºC, below the melting point of lanoline (36-42ºC). Two variables are studied, the extraction pressure and the solvent mass flowrate. Our model depends on three parameters: the solubilities of the two lanoline fractions and the lanoline mass transfer coefficient. The model is a set of first-order partial differential equations, that is solved by orthogonal collocation in combination of optimization of the parameters. The fluid-side mass-transfer coefficient decreases with extraction pressure and is about 5 x 10^{-6} m/s for Re < 1 (at 70 -150 bar) and depends on fluid velocity. The solubilities of lanoline fractions, independent of flowrate, agree very well with those previously reported.

Nomenclature: See end of the manuscript.

1.Introduction

Lanoline is a natural wax secreted by the sebaceous glands of sheep that finds valuable applications in pharmacy and cosmetics [1-2]. Lanoline is traditionally obtained from raw wool by washing the sheep with water and soap. For pharmaceutical and cosmetic applications, however, it cannot be used directly, as it requires a complex purification process. An interesting alternative is to use a waterless washing with high pressure carbon dioxide, either neat [3,4] or modified with co-solvents [5,6], in the liquid state or as supercritical fluid. This paper focuses on the high pressure extraction of lanoline from raw wool under near-critical conditions with ethanol-modified CO_2, using our previously published experimental results [6, 7].

Among the first authors to study SCF applied to lanoline extraction from raw wool are King and coworkers [3], Koo at al. [5] as well as New Zealand researchers [3]. These authors used neat CO_2 in their studies. Shortly later, we filed a patent [7] based on the fractionation of lanoline lipids using compressed CO_2, using either raw wool or technical lanoline as a starting material, with a solvent based on modified CO_2 [7]. Solvent-modified CO2 under quasi-critical conditions is faster than neat CO2 [6,7] requiring less pressure and temperature.

In the present paper, we specifically focus on the two lanoline fractions obtained in the process of Bayona et al. [7] and the evidence about their existence provided in our previous work [6]. Bayona found that there are two fractions: 1) A lanoline soluble in the cosolvent, that is highly polar and has a narrow molecular weight, and 2) Another lanoline fraction insoluble in the cosolvent, that has a wide molecular weight distribution. More recently, further characterization have been made [8-10].

Particularly important are the experimental results published by our group [6], as they form the basis of the present study. We carried out experiments to find the best cosolvent concentration and the extraction kinetics using subcritical and supercritical solvent. The effects of temperature, pressure, fluid velocity and wool compression were examined experimentally. In all cases, an extracted lanoline fraction appeared at low contact time, followed by a second fraction. Theses fractions are those found in the process of Bayona et al [7]. According to our findings [6], the best extraction conditions of raw wool are with a near-critical solvent with 5% ethanol, and with a contact time corresponding to a specific mass flowrate of 10-25 kg/h/L. Runs carried out at a very slow fluid velocity were also done by Eychenne et al [6]. These runs in which saturation conditions prevailed, indicated the existence of the two lanoline fractions. Their previously reported solubilities [6] are one of the objectives to verify in the present work.

We had two purposes in this article. First, focusing on the two fractions of lanoline discussed above, we used the shrinking-core concept to describe lanoline extraction kinetics from raw wool. So that the solid lanoline is in contact with the fluid. Therefore, the only mass transfer resistance that exists is the individual fluid-side mass-transfer coefficient. Secondly, in order to solve the extraction model, the orthogonal collocation method was applied to solve a system of nonlinear first-order partial differential equations. This is used to determine the extracted fraction of lanoline as a function of time.

2. Experimental background

The experimental study behind this work was published earlier in this journal [6]. Here we report only the most significant features. The detailed process flow diagram for the high-pressure extraction setup is shown in Fig 1 A summary of the

experimental scope of the measurements, the extractor unit, the wool stock used, and the solvent properties, is given on Tables 1, 2, and 3.

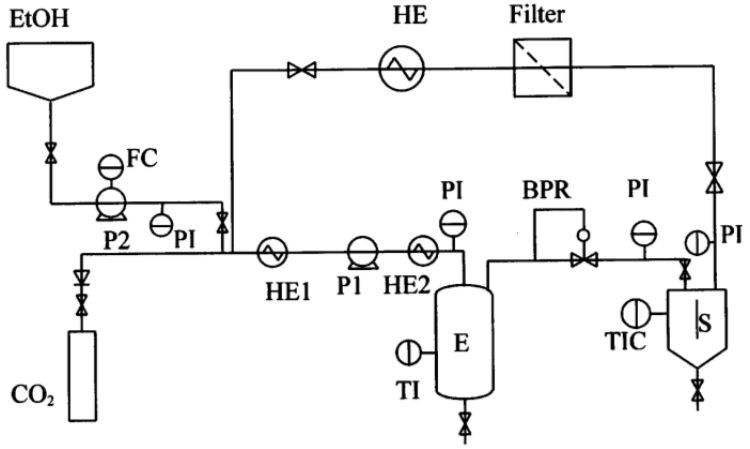

Fig.1. Separex 200 unit process flow diagram. P1, Milton-Royal CO_2 pump; P2, Pulsa-Feeder ethanol pump; HE1, HE2, HE3, heat exchangers; BPR back-pressure control valve; E, Separex 200 extractor; S, Separex cyclone separator; PI, pressure indicators; TIC temperature indicating controller; FC, flow controller

Table 1. Scope of the measurements

Temperature	30 ºC
Pressure	70, 120,150 bar
Type of solute	Lanoline
Solvent mass flow rate, $\dot{m}$	3 – 4 kg/h
Total extraction time	8000 s
Solvent passed	0 – 6,6 kg
Solvent composition, % wt	95% CO_2 – 5% ethanol
Wool packing density, ρ_B	126,8 kg/m^3

Table 2. Properties of extractor and wool

Extractor vessel	
Type	Separex SCF 200
Material	Stainless steel AISI 316L
Cylinder inside dimensions	145 mm x 30 mm (H x D)
Volume	100 cm^3
Cross section	706,8 mm^2
Wool fibers	
Wool load	13 g
Wool composition	60-65% wool proper, 10-15% wax and proteins, 10% soluble stains (salts), 1-20% soil and vegetable matter
Fiber geometry	Cylindrical

Fiber length (approx.)	15 cm
Diameter of fiber, D	20 μm
Lanoline content	15-30% wt
Types of lanoline	Two lanoline fractions (external and internal)
Lanoline melting point, T_m	38 – 44 ºC
Calculated wool fiber properties	
Initial fiber radius, r_0	10 μm
Change of lanoline fraction radius, R^{*a}	9,5 μm
Final fiber radius, R	8,9 μm
Raw wool density, ρ_w	1314 kg/m^3
Lanoline density, ρ_l	940 kg/m^3
Bulk density, ρ_B	126,8 kg/m^3
Bed porosity, ε	0,9
Fiber Sauter particle size, [b]	3 x 10^{-2} mm

[a] See paragraph 3.1, [b]Valverde [11]

Table 3. Properties of solvent, 5%EtOH-95%CO_2

Tc	37,4 ºC
Pc	77,3 bar
Solvent density, ρ_s	783,3 kg/m^3
Viscosity, μ *	0,0648 mPa.s

* Fields et al. [12].

In our previous work [6] the effect of various variables on the extracted lanoline vs. time with modified CO_2 is shown. The effect of ethanol concentration, was studied (from 5% to 30% ethanol), and the lower % of ethanol chosen for economy. The raw wool employed contained 15% wt of lanoline. In our previous paper, it was reasoned that extraction of lanoline takes place in two successive steps. This corresponds to the two lanoline fractions located one over the other on the wool fibers, rather than to a wax mixture or fractions adsorbed on different sites. This is consistent with the fractions observed earlier in our patent [7] and in [6], as reasoned in the Introduction section. In a previous paper [6], we showed that the best temperature for desorption of lanoline is 30ºC. At this temperature, the lanoline layer on wool is a solid and the fluid is a near-

critical liquid. On Fig 2 is the PT diagram for the 5% ethanol-95% CO_2. For 30ºC and pressures of 70-150 bar, the solvent is a liquid. In the present paper, extraction at a single temperature of 30ºC is considered, where extraction is fastest, and the lanoline layer is a solid in contact with the fluid.

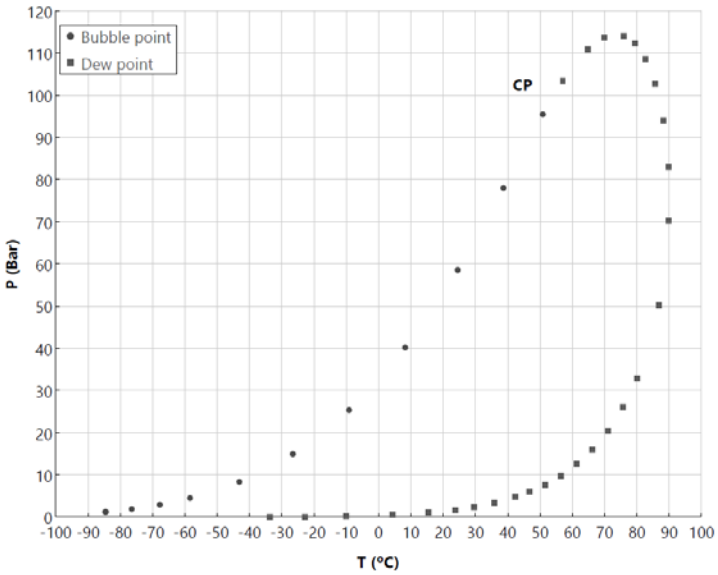

Fig 2. PT diagram for the mixture 5% ethanol-95% CO2. CP is the critical point. For T= 30ºC and pressures above 70 bar, the fluid is a liquid.

3. Extraction model

3.1 Previous findings to consider in the model.

As will be discussed in the model, the radius of the wax layer where lanoline fraction changes, is a key parameter of the model. Eychenne et al. [6] performed extraction runs at very low velocity runs to determine the approximate lanoline solubility at different pressure and temperature conditions. By plotting the mass of solute extracted vs. mass of fluid passed, the slope of the graph allows to estimate the approximate solubilities of lanoline fractions in the solvent. From these experiments, it can be clearly seen the two lanoline fractions, suggesting that one desorbs after the other, and that the first fraction has a larger solubility than the second one. The break

point of the total curve with different slopes, can be used to calculate the radius at which the change of fraction occurs. On Fig 3, we give the regression lines of the equilibrium plots for 30ºC and 150 bar.

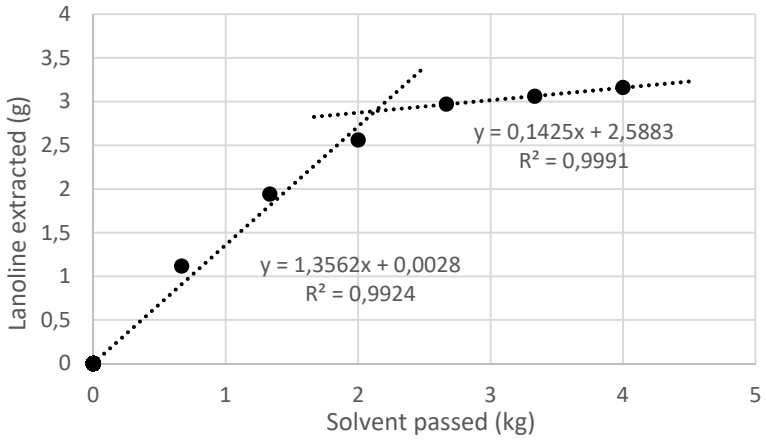

Fig 3. Extraction run at very small fluid velocity. Data points are from [6], showing the extraction of the two lanoline fractions. Regression of solubility data to obtain the intersection point (T = 30 ºC, P =150 bar, wool packing density 390,3 kg/m^3). The slopes of the straight lines give the solubilities in g/ kg fluid.

Fig 3 provides the radius of the lanoline, R*, where the change occurs, by the following calculation. Let N_f be the total number of wool fibers in the extractor, m_{wool} = 40 g, and the lanoline mass extracted at the break point, $m_{extracted}$ = 2,892 g (from Fig 3).

Therefore, for a cylindrical wool fiber, we can write:

$$\frac{N_f \pi (r_0^2 - R^{*2}) \rho_l}{N_f \pi r_0^2 \rho_w} = \frac{m_{extracted}}{m_{wool}} \qquad (1)$$

Hence,

$$R^* = r_0 \sqrt{1 - \frac{m_{extracted}}{m_{wool}} \frac{\rho_w}{\rho_l}} = 10 \sqrt{1 - \frac{2{,}892}{40} \frac{1314}{940}} = 9{,}48\ \mu m$$

Also, a simple calculation allows to establish the final radius, R, at which the lanoline has been completely extracted. The raw wool is known to contain, on average, 15-30% wt, of lanoline . After a few runs with the model it is clear that the exact % is in our case 15%, so that , $m_{lanoline}/m_{wool}$= 0,15. Then, we have:

$$\frac{N_f \pi (r_0^2 - R^2)\rho_l}{N_f \pi r_0^2 \rho_w} = \frac{m_{lanolin}}{m_{wool}} \qquad (2)$$

From which,

$$R = r_0 \sqrt{1 - \frac{m_{lanolin}}{m_{wool}} \frac{\rho_w}{\rho_l}} = 10 \sqrt{1 - 0{,}15 \frac{1314}{940}} = 8{,}89\ \mu m$$

3.2 Mass conservation equations for lanoline.

3.2.1 Conservation in the fluid phase.

We first write the conservation equation for lanoline solute in the fluid phase, and then, on the solid phase. Let us call r_v the volumetric rate of lanoline desorption in the fluid. For the general case of disperse fluid flow in the z-direction, the conservation of lanoline over a differential bed length dz, leads to the following equation:

$$\varepsilon \frac{\partial C}{\partial t} + u \frac{\partial C}{\partial z} = D_z \frac{\partial^2 C}{\partial z^2} + r_v \qquad (3)$$

Where C is the lanoline concentration in the fluid at a position z, and time t. For a packed bed of 15 cm long, with wool of equivalent particle size of less than 1 mm (see Table 1), the equivalent number of perfect mixers in series is very large, and, consequently, $Pé_z >> 100$, so plug flow conditions can be assumed. So, eq. 3 can be written as:

$$\varepsilon \frac{\partial C}{\partial t} + u \frac{\partial C}{\partial z} = r_v \qquad (4)$$

Where r_v is the solid-to-fluid mass transfer rate:

$$r_v = k_g a (C^* - C) \qquad (5)$$

In which, it is assumed that the fluid-phase concentration of lanoline close to the solid in contact with the solvent is *C**, and *a* is the specific surface of wool fibers per unit

volume of bed. If r is the cylindrical fiber radius and L its length, the area *a*, can be can be written as:

$$a = \frac{2\pi rL}{\pi r^2 L}(1-\varepsilon) = \frac{2(1-\varepsilon)}{r} \qquad (6)$$

With *a* from eq (6) into eq (4), this becomes:

$$\varepsilon \frac{\partial C}{\partial t} + u\frac{\partial C}{\partial z} = k_g \frac{2(1-\varepsilon)}{r}(C^* - C) \qquad (7)$$

Where *r* is a function of time and position in the bed z, i.e., r (t, z). Note that the void fraction, ε , in eq (7) is in fact variable with time because the lanoline dissolves into the fluid leaving a thinner film.

3.2.2 Conservation of lanoline in the wool phase

To describe extraction kinetics, we apply the concept of the shrinking-core model (SCM) with a cylindrical geometry. Refer to the radius shown on Fig 4.

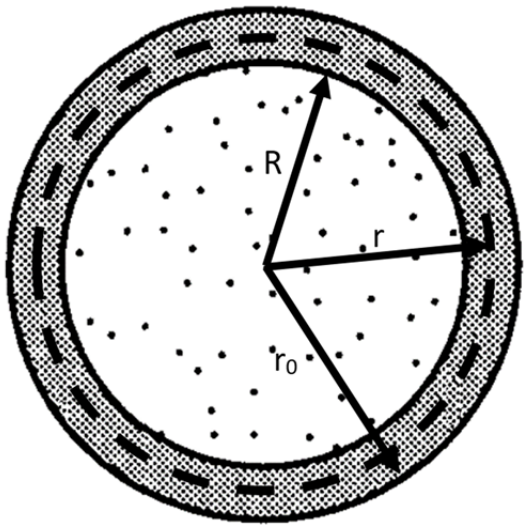

Fig 4. Shrinking-core model for a cylindrical lanoline cover on wool fiber. Initial external radius is r_0, inner radius is R, and variable dotted line is the shrinking radius r.

Whereby, the lanoline mass on a fiber of length L, at time t and position z in the bed, will be:

$$m_f = (\pi r^2 - \pi R^2) L \rho_l \qquad (8)$$

The number of fibers initially loaded in the bed (assumed cylindrical) is given by:

$$N_f = \frac{(1-\varepsilon_0)\pi {R_B}^2 Z_t \rho_w}{\pi {r_0}^2 L \rho_w} = \frac{(1-\varepsilon_0){R_B}^2 Z_t}{{r_0}^2 L} \qquad (9)$$

Where R_B is the bed radius and Z_t is the bed length. In eq (9), ε_0 is the initial bed porosity, and r_0 the initial raw wool fiber radius. See other symbols in the Nomenclature section. With this, the initial mass of lanoline present in the packed bed, will be:

$$m = N_f m_f = \frac{\pi \rho_l (1-\varepsilon_0){R_B}^2 Z_t}{{r_0}^2}(r^2 - R^2) \qquad (10)$$

Differentiating *m* with respect to t in eq (10), and dividing by the total bed volume, V_B, we will have:

$$\frac{\partial m}{V_B \partial t} = \frac{2\rho_l (1-\varepsilon_0) r}{{r_0}^2}\frac{\partial r}{\partial t} \qquad (12)$$

Now, equating eq (12) and eq (5) with a minus sign, we obtain the change of radius r with time, as:

$$\frac{\partial r}{\partial t} = -\frac{k_g}{\rho_l}\frac{(1-\varepsilon)}{(1-\varepsilon_0)}\frac{{r_0}^2}{r^2}(C^* - C) \qquad (13)$$

In summary, the model equations for the extraction of the lanoline is represented by the following system of equations:

$$\frac{\partial C}{\partial t} = \frac{2k_g}{r}\frac{(1-\varepsilon)}{\varepsilon}(C^* - C) - \frac{u}{\varepsilon}\frac{\partial C}{\partial z} \qquad (14a)$$

$$\frac{\partial r}{\partial t} = -\frac{k_g}{\rho_l}\frac{(1-\varepsilon)}{(1-\varepsilon_0)}\frac{{r_0}^2}{r^2}(C^* - C) \qquad (14b)$$

A refinement of the model is possible. The value of ε_0 is the initial porosity of the wool bed employed to calculate N_f with eq. (9). Note, however, that the bed void fraction

increases because of the extraction of the lanoline due to its extraction to the fluid. In the above equations, ε is the porosity at time t and radius r. The two porosities are related through the following equations:

$$\varepsilon_0 = 1 - \frac{\rho_B}{\rho_w} \qquad (15)$$

$$\varepsilon = 1 - \frac{\rho_B}{\rho_w}\frac{r^2}{{r_0}^2} \qquad (16)$$

With these expressions substituted into eqs. (14), the model equations become:

$$\frac{\partial C}{\partial t} = \frac{2k_g(1-\varepsilon_0)r(C^* - C) - u{r_0}^2\frac{\partial C}{\partial z}}{{r_0}^2 - (1-\varepsilon_0)r^2} \qquad (17)$$

$$\frac{\partial r}{\partial t} = -\frac{k_g}{\rho_l}(C^* - C) \qquad (18)$$

This is a system of two coupled nonlinear partial differential equations.

For the initial conditions, it is considered that initially the extractor contains no fluid, so that the lanoline concentration in the fluid is zero at all positions, and the initial radius of lanoline is r_0 everywhere. In this idealized model, when solvent is allowed into the bed (t = 0), an instantaneous compression of the bed takes place with C = 0. For the boundary conditions, it is assumed that at bed entrance (z = 0) the fluid has no lanoline, so C = 0. Therefore, the initial and boundary conditions for C (t, z) and r (t, z), are:

$$C(0,z) = 0$$

$$r\,(0,z) = r_0 \qquad (19)$$

$$C(t,0) = 0$$

3.3 Dimensionless mass transfer model.

In order to make the model non-dimensional we define the following variables:

$$Y = \frac{C}{C_1^*}$$

$$Y^* = \frac{C^*}{C_1^*}$$
$$\eta = \frac{r}{R} \qquad (20)$$
$$x = \frac{Z}{Z_t}$$
$$\tau = \frac{t}{\theta}$$

Where the first lanoline fraction, whose solubility is C_1^*, is the first solute to be extracted. With the new variables, the model becomes:

$$\frac{\partial Y}{\partial \tau} = \frac{2\psi(1-\varepsilon_0)\eta(Y^*-Y)-\eta_0\frac{\partial Y}{\partial x}}{\eta_0^2-(1-\varepsilon_0)\eta^2} \qquad (21)$$

$$\frac{\partial \eta}{\partial \tau} = -\xi\psi(Y^* - Y) \qquad (22)$$

Where Y is the solute concentration in the fluid, η is the fiber radius relative to R, and τ is the dimensionless time. See the other symbols in the Nomenclature. The initial and boundary conditions for eqs. (21) and (22), are now:

IC:

$$Y(0,x) = 0$$
$$\eta(0,x) = \frac{r_0}{R} \qquad (23)$$

BC.

$$Y(\tau,0) = 0 \qquad (24)$$

The system of eqs. (21) to (24) allows the method of orthogonal collocation to be applied in the x-domain [0,1], thus simplifying the solution (see paragraph 4). We now describe the conditions at the fluid-solid interphase as respect to the two lanoline fractions.

*3.4 Lanoline concentration profile and the change radius called R**

As has been reasoned, the lanoline fractions is deposited on the wool fiber forming two coaxial cylindrical layers. These have different but well-defined solubilities. At T = 30ºC, they are solid. Neglecting the solubility of the fluid in the solid, diffusional effects in the lanolin layer do not take place. Refer now to Fig 5.

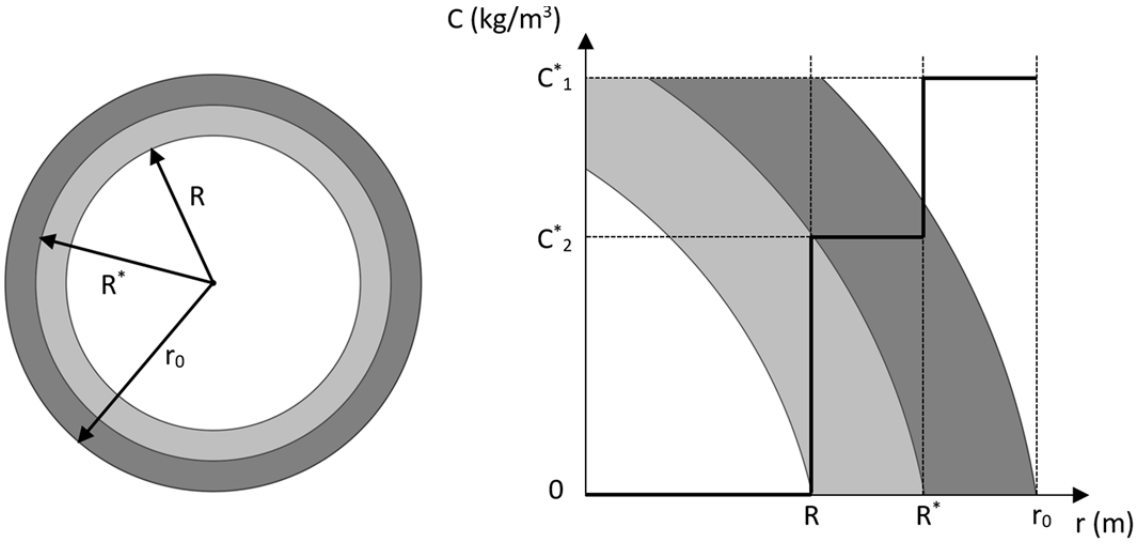

Fig 5. Solid lanoline solubility profile on the fiber. The change radius R*, separates the two lanoline fractions.

Based on the position of solute on the fiber, a concentration profile of C* in a double step is considered, in such a way that C_1* is constant from the initial radius r_0, up to the change radius R* , where the second lanoline fraction is reached. From this radius inwards, the saturation value C^*_2 is constant again up to the point where the radius occupied by lanoline becomes zero. In order to mathematically include the step function in the saturation values, the following continuous function is used [13]:

$$u(t) = \frac{1}{1 + e^{-\alpha t}} \qquad (25)$$

The use of the exponential function is justified by the need to introduce a step expression with a continuous derivative so numerical problems are avoided. In eq. (25), an appropriate large value for α is used. In the non-dimensional model, eqns. (21) and

(23), the core radius η, takes values comprised between r_0/R and 1, while the fluid concentration Y, takes values between 1 and 0. Therefore, the initial step for the extraction will take a value C_1^*/C_1^* during the first fraction extraction, hence, u(t) = 1. The second step will take a value C_2^*/C_1^*, when the radius is η = R*/R.

In order to introduce a double step like that of Fig 5 in the model equations, it is necessary to write a value Y*(η) containing the two different limits. This is done in the following way:

$$Y^*(\eta) = \left(\frac{1 - Y_{12}^*}{1 + e^{-\alpha(\eta-\eta^*)}} + Y_{12}^*\right)\left(\frac{1}{1 + e^{-\alpha(\eta-1)}}\right) \qquad (26)$$

Where $Y^*_{12} = C^*_2/C^*_1$, and η* = R*/R. In the calculations, a large value for α is given, for example, $\alpha = 10^{1000}$.

4. Solution of extraction model and parameter optimization

4.1 Orthogonal collocation

In order to solve eqs. (21-24), the method of orthogonal collocation (OC) [14-16] is proposed. As shown by early authors, the OC method is faster and more accurate than most finite difference methods for PDE systems [15,16]. The method is based on approximating the trial solution consisting in a sum of orthogonal polynomials with initially unknown coefficients. We express the solution to Y and η as a function of time τ only. In such a way that when the trial solutions are substituted in the system, the partial derivatives with respect to τ become total derivatives and the partial derivatives with respect to x, which are Y and η, form a matrix of values for different points of the bed (the collocation points). As a result, the system of equations become a system of initial-value ODEs with respect to τ that is readily solved with standard methods

(Runge-Kutta, Gear, etc). The trial functions in our case can be written in terms of the polynomials, in a simple manner, as:

$$Y(\tau,x)=\sum_{i=0}^{N} a_i(\tau)P_i(x)$$
$$\eta(\tau,x)=\sum_{i=0}^{N} b_i(\tau)P_i(x) \qquad (27)$$

The orthogonality condition for two polynomials with respect to a weighting function, w(x), in the interval [a, b], is:

$$\int_a^b w(x)P_n(x)P_m(x)dx = C_{(n)}\delta_{nm} \qquad (28)$$

Where $C_{(n)}$ is a normalizing factor, and δ_{nm}, is Kronecker´s delta. In our case, only the polynomials derived from the Rodrigues´ formula [18]were considered, so it guarantees the orthogonality condition. In practice, the Legendre polynomials, orthogonal in the the [0,1] x- interval, were used. Its series expression has been used here to calculate the coefficients with MATLAB (see dimensionless model in paragraph 3.3).

The form of the trial functions used in the present work are those used by Villadsen and Stewart [14] and later by Finlayson [15]. They are:

$$Y(\tau,x)=Y(\tau,1)+(1-x^2)\sum_{i=0}^{N-1} a_i(\tau)P_i(x^2)$$
$$\eta(\tau,x)=\eta(\tau,1)+(1-x^2)\sum_{i=0}^{N-1} b_i(\tau)P_i(x^2) \qquad (28)$$

In these expressions the polynomials are the same but in terms of x^2, so even polynomials are obtained, hence with symmetrical solutions. Therefore, they are useful in problems with a symmetric geometry (slab, cylinder, sphere). The number of collocation points is N+1, that is, equal to the number of polynomials employed. The

collocation points are the roots of the polynomial of highest degree [14,17]. In this case, x = 0 and x = 1 are both taken also as collocation points, as a boundary condition is set at x = 0 and the solution is wanted at x =1. In our calculations, we employed the Legendre polynomials with even exponents, because they give the least oscillations, and they are easily constructed with MATLAB.

4.2 Optimization of parameters

After the solution of the extraction model is obtained in terms of the fluid phase concentration at bed exit, it is necessary to characterize the system parameters from the experimental data available [6]. These results are usually given in terms of the lanoline fraction extracted as a function of time at the bed exit, hereinafter called X(t). To calculate X from the solution of the model, the following expression is used:

$$X(t) = \frac{\int_0^t C(t, Z_t)dt}{\int_0^\infty C(t, Z_t)dt} \qquad (29)$$

To calculate the fraction extracted as a function of time, the following change of scale is done: $m_s = m't$, where m' is the mass flow rate of solvent.

The optimization function used to obtain the parameters, is that employed previously by Valverde at al.[19], based on the squared relative deviations of extracted fractions, as:

$$FO = \sum_{i=1}^{n} \left(\frac{X_i^{exp} - X_i^{model}}{X_{max}^{exp}} \right)^2 \qquad (30)$$

In eq. (30), n is the number of data points at a given pressure (for 70 and 120 bar, n = 6; and for 150 bar, n=5). The global optimization algorithm used was *Genetic Algorithm* (GA) available in MATLAB, because the local optimization methods performed quite

inefficiently. GA instead provides precise and optimal results with problems with poor flexibility as discussed elsewhere [19].

5. Results and discussion

5.1 Experimental data available

The experimental data used for modeling are those of Eychenne et al. [6]. Mainly, from the figures 4 6a and 9a, at 30ºC, of that article [6]. Shown on Tables 4 and 5, are the Eychenne results for extraction at different pressures and mass flowrates. In what follows, we first discuss the parameters and identify their relative sensitivity. Then, we discuss the results obtained for the fitted parameter values as a function of the extraction pressure. And finally we present the effects of flowrate on the parameters.

Table 4. Effect of pressure on extracted fraction vs. time. Experimental data from Eychenne et al. [6]. (T = 30 ºC, flowrate m´= 4 kg/h, ρ_B = 126,8 kg/m^3).

Solvent passed [kg]	Lanoline extracted fraction		
	70 bar	120 bar	150 bar
0,67	0,24	0,28	0,34
1,33	0,45	0,53	0,61
2,0	0,64	0,68	-
2,67	0,70	0,78	0,86
3,33	0,76	0,84	0,93
4,0	0,85	0,87	0,97

Table 5. Effect of solvent flowrate on extracted lanoline vs. Time. Experimental data from Eychenne et al.[6] . (T = 30 ºC, P = 120 bar, ρ_B = 126,8 kg/m^3).

Solvent flowrate			
3 kg/h		4 kg/h	
Solvent passed [kg]	Lanoline extracted fraction	Solvent passed [kg]	Lanoline extracted fraction
0,75	0,46	0,67	0,32
1,5	0,59	1,33	0,55
2,25	0,77	2,0	0,71
3,0	0,8	2,67	0,81
		3,33	0,84

5.2 Model parameters and their sensitivities

In our system model, eqs. (21)-(24), there are three parameters to fit together. Apart, there is the change radius R*, that is well established (see Paragraph 3.1). The three unknown parameters are the values of the solubilities of the lanoline fractions C_1* and C_2*, and the value of the fluid-side mass transfer coefficient k_g. It is interesting to note that in the present problem the geometry and size of wool fibers are well defined, so that a value of k_g is obtained separately from the transfer area. Approximate values of the lanoline solubilities are available (see Fig 3) that can be used as a guide to verify the validity our results.

We first examine the sensitivity of the objective function FO, eq. (30), to the parameters. The results can be seen on Fig 6 where the response of the fraction extracted is simulated when parameters are changed one at a time.

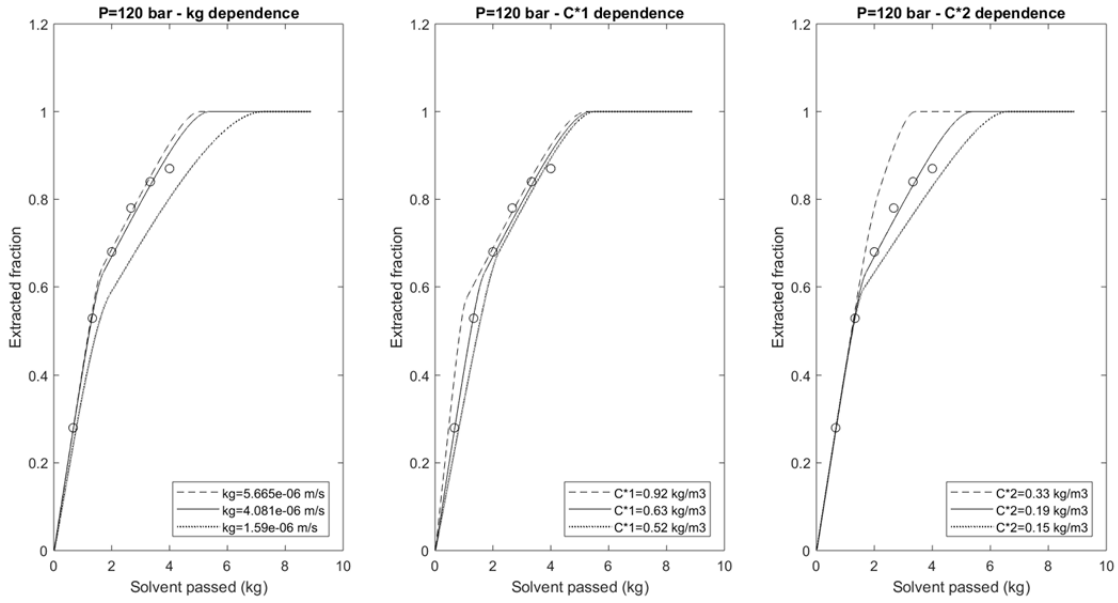

Fig 6. Simulated extracted fraction vs. solvent passed when parameters are varied (T = 30 ºC, P = 120 bar, m´= 4 kg/h). Data points are from [6].

Fig 6 reflects their relative influence. The value of C_1* shows a large effect on the first part of the response curve, while C_2* shows it higher effect on the second part of the curve. This was expected from the two lanoline fraction involved. Also, it is seen that when k_g and the solubilities are both diminished, the response curve is shifted to the right or to larger extraction times. The most important feature of Fig 6 is the individual effect of each parameter.

The order of importance is as follows. A slight change in C_2* has the larger effect on the model solution, so this parameter is the most sensitive. The next influential parameter is k_g, and finally the least influential is C_1*, but it is still important. As a consequence, the response curve is good enough for determining the three model parameters as all three affect the extraction rate.

5.3 Results on the pressure dependence

Combining the solution of the model with parameter optimization, the resulting values of k_g, C_1* and C_2* are obtained, and given on Table 6, where the effect of extraction pressure is clearly seen.

Table 6. Final values of parameters at 70, 120 and 150 bar (30 ºC and 4 kg/h flow rate).

	70 bar	120 bar	150 bar
k_g (m/s)	$5{,}66\cdot10^{-6}$	$4{,}08\cdot10^{-6}$	$1{,}59\cdot10^{-6}$
C_1^* (g/kg solvent)	0,665	0,807	1,178 (1,35)[b]
C_2^* (g/kg solvent)	0,194	0,242	0,427 (0,47)[b]
FO[a]	0,00071	0,00315	0,00105

[a]Minimum of objective function. [b]Values in parenthesis are the solubility values measured by Eychenne et al. [6] (see Fig 3).

As can be observed, the values of the solubilities C_1* and C_2* at 150 bar, agree very well with those measured previously [6]. The effect of pressure on the solubilities between 70 and 150 bar is the expected result. Also, the fluid-side individual mass transfer coefficient k_g, is seen to decrease with increasing pressure, in agreement with Brunner [20], and to those found experimentally by other authors [21,22].

It is interesting to note that k_g has been obtained independently of the transfer area. Note also that its measurement is free from other mass transfer resistances that usually accompany mass transfer studies (see liquid-to-supercritical fluid mass transfer studies, [21]). The value of k_g obtained can be compared using the publication of Puiggené et al [21] where the global K_g measured by several SCF authors are represented as a function of Reynolds number. The range of the particle Reynolds number in our experiments [6] is around Re ~ 0,7 (Re = 0,65-0,72) with a value of the k_g (Table 6) in the order of 5 x 10^{-6} m/s (for P = 70-120 bar). This value is similar to the mass transfer coefficient found by Tan et al. [22], also at the interphase solid-fluid, for the case of packed-bed desorption with SCF.

On Fig 7, the evolution of the lanoline fluid concentration and the wool fiber radius as a function of time, are presented for the pressures of the study, using 20 different collocation points along the bed. On the left of the figure, are the graphs of C(t, z) vs. time, and on the right are the fiber radius r (t,z), using the Legendre polynomials.

Some features of Fig 7 deserve comment. Because the first lanoline fraction extracted is more soluble, the radius drops sharply (see left side of Fig 7) for a change radius of R* = 9,5 mm. This sharp drop is a characteristic feature of SCM kinetics for gas-solid reactions [24]. Because the second lanoline fraction is less soluble, the radius r (t) for r = R* drops also to a constant final value for r = R (all lanoline extracted). This is seen very clearly on Fig 7.

As regards to the lanoline concentration in the fluid, graph of C vs. t, the stepped profile at bed exit is due to the steps in the radius and to the solubility. These steps can be smoothed by using more collocation points in the model. However, the concentration graph at bed exit, presents a response with more steps.

In Fig 8 the steps have been eliminated, and continuous lines for the concentration and the radius vs. time can be seen. The general trend with extraction pressure is clearly apparent on Fig 8.

As a final result, the corresponding extracted fraction of lanoline vs. solvent passed is given on Fig 9, where the effect of pressure on extraction kinetics is calculated with our model with the optimum parameter values of Table 6, and with the experimental data [6]. As can be observed on Fig 9, the best extraction conditions at 30ºC correspond to 150 bar.

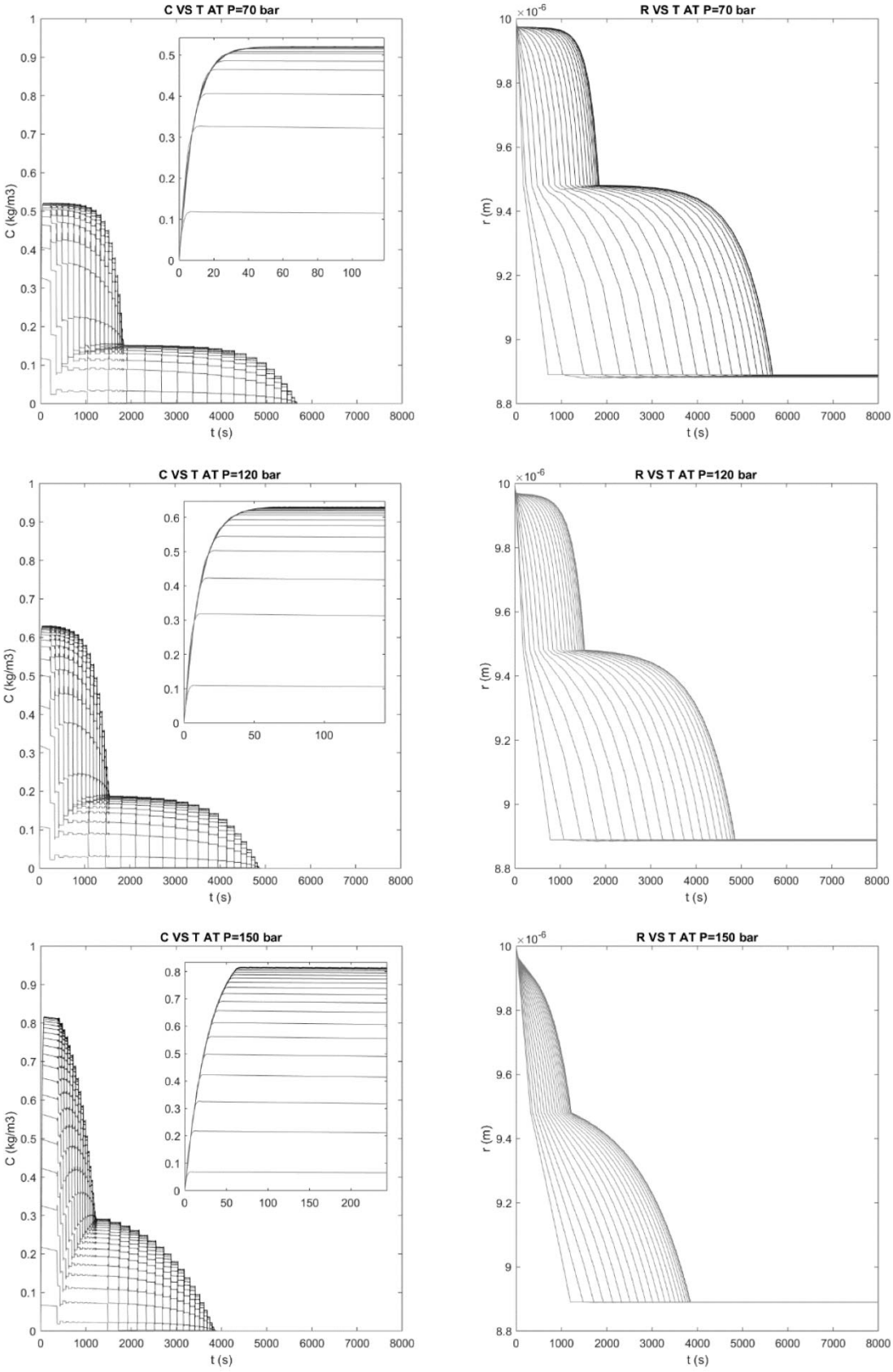

Fig 7. Time evolution of lanoline concentration in the solvent (left) and radius of the fiber (right), for extraction at 30 ºC and w´= 4 kg/h flow rate, for 20 different collocation points along the bed. The leftmost lines (clearer lines) show the evolution of lanoline concentration at a point near the extractor entrance while the right lines (darker ones) are for points near the exit.

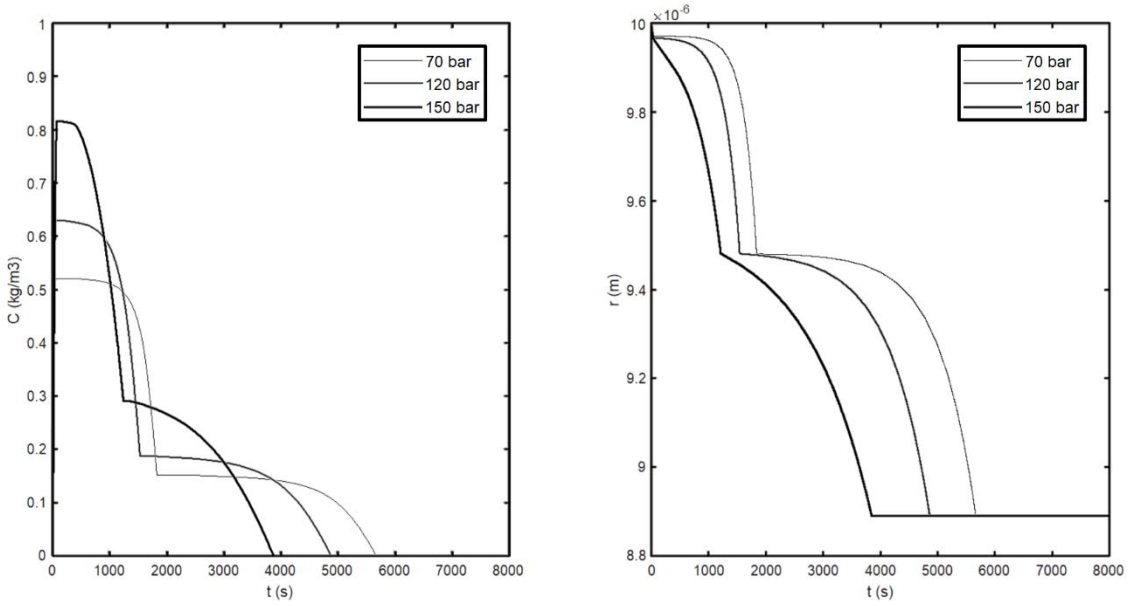

Fig 8. Calculated concentration of lanoline in the solvent (left) and radius of the fiber (right) evolution with time at the extractor exit, as a function of pressure (30 ºC and m´= 4 kg/h)

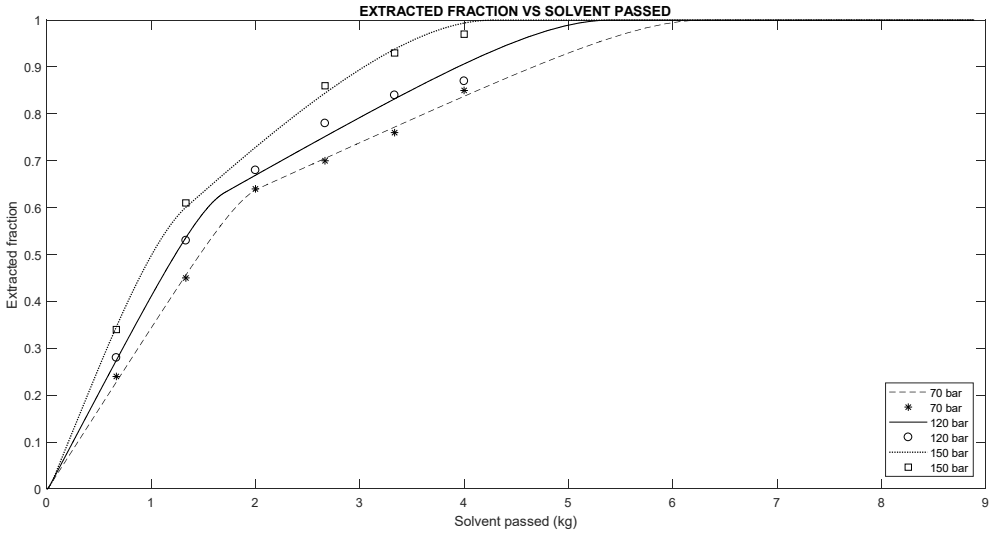

Fig 9. Fraction extracted vs. solvent passed at 70 bar, 120 bar and 150 bar, (30 ºC and m´= 4 kg/h) Data points are from [6], continuous lines with our model with best parameter values (Table 7). Best extraction conditions are 30ºC and 150 bar.

5.4 Results on flowrate dependence

After obtaining the parameters k_g, C_1*, and C_2* by modeling the experimental results of Eychenne et al [6] , the fitting of the model parameters was done for the two fluid

velocities for which extraction data are also available. The results are summarized on Table 7. These show the effect of increasing the solvent flowrate from 3 kg/h to 4 kg/h for runs at constant T and P (30ºC and 120 bar).

The solubility values C* should be independent of the flowrate because solubilities are thermodynamic properties, thus they depend on temperature and pressure only. This is the behavior observed for C_1* (C_1* = 0,242 g/kg, Tables 6 and 7), hence with good agreement. For the case of C_2* the agreement is fair, as there is a slight difference between the values of Tables 6 and 7 (C_2* = 0,807 g/kg in Table 6 vs C_2* = 0,853-1,149 g/kg in Table 7). Anyway, these values agree within an order of magnitude.

As regards to the mass transfer coefficient k_g, this is seen to increase by 25% with an increase in fluid velocity of 33%, see Table 8. The observed increase implies a dependence of k_g on velocity as $u^{0,77}$. In general, for gas flow and liquid flow in packed beds, the dependence of a fluid side mass transfer coefficient k_g on the velocity is taken into account through correlations of the type Sh vs. Re. For SCF, for example, Tan et al.[22] found a correlation of the type, $Sh = 0{,}38\, Re^{0,83} Sc^{1/3}$ (Re = 2-40) with an exponent 0,83, larger than the exponent accepted today for packed beds (0,65) but closer to our exponent 0,77. Unfortunately, we do not have enough results at larger velocities to establish the velocity exponent with more precision.

On Fig 10, the fraction of lanoline extracted vs. time for increasing mass flowrates, is presented [6]. As reasoned above, a dependence of k_g on $u^{0,77}$ would require to examine a wider flowrate range to see its effects reflected on the extraction rate, that are hardly seen on Fig 10.

Table 7. Effect of flowrate on optimized parameters for 3 kg/h and 4 kg/h flow rate (120 bar and 30 ºC.)

	3 kg/h	4 kg/h
k_g (m/s)	$4{,}09 \cdot 10^{-6}$	$5{,}13 \cdot 10^{-6}$
C_1^* (g/kg solvent)	1,149	0,853
C_2^* (g/kg solvent)	0,236	0,256
OF	0,00703	0,00422

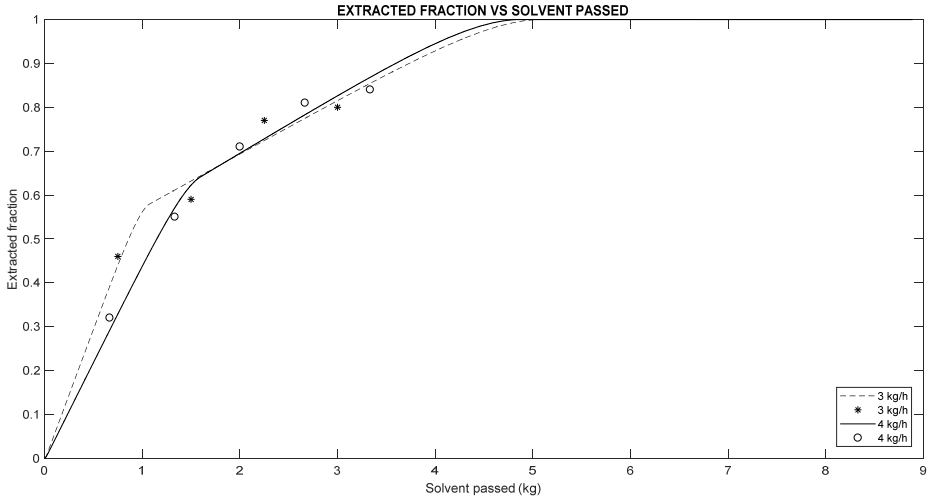

Fig 10. Effect of flowrate of the fraction of lanoline extracted vs. solvent passed (3 and 4 kg/h, 30 ºC and 120 bar). Experimental data points are from [6], continuous lines with our model with best parameters of Table 7.

6. Conclusions

Using our previous publications, on the experimental results of near-critical extraction of lanoline from raw wool with modified carbon dioxide, a mass transfer model has been developed that explains extraction kinetics at 30ºC, below the melting point of lanoline. That is, at conditions where the lanoline is a nonporous solid and the solvent is a compressed liquid. Our model assumes that the two lanoline fractions deposited one over the other on the wool fibers. This picture is suggested by our previous findings and a patent. When extraction starts, the first lanoline fraction to be dissolved is that on the outer layer in close contact with the fluid. Afterwards, a less soluble second fraction is extracted. The first fraction has a higher solubility, while the second one is less soluble. A critical or change radius, denoted R*, that characterizes the

transition from one fraction to the other, was measured and is taken a as key data in the model.

The extraction model proposed is based on the shrinking-core model for solid-fluid reactions, with a cylindrical particle geometry. Because, the mass transfer area for lanoline dissolution is relatively well defined, the only rate coefficient for lanoline extraction is the individual fluid-side coefficient, k_g, a value for which was calculated here. The extraction model depends on two additional parameters. These are the solubilities of the two lanoline fractions. The model performs very well in describing the extraction kinetics observed, in particular, the dependence on the extraction pressure and the solvent mass flowrate.

In order to solve the system of nonlinear first-order partial differential equations that appear in the model, the method of orthogonal collocation, as developed by the early authors (Villadsen and Stewart, and Finlayson), has been used here. In this way, we have chosen the Legendre polynomials that gives a solution with least oscillation. The solution of the extracted lanoline and the radius of remaining lanoline on the fiber as a function of time, allows to obtain the model parameters. These are obtained using a global optimization procedure combined with the solution of the mass transfer model.

Nomenclature

a	Specific surface area, m^2
a_i, b_i	Coeffs. of polynomial P, eq 26
C	Lanoline conc. in solvent, kg/m^3
C^*	Solubility, kg/m^3
C_1^*	Solubility of fraction 1, kg/m^3
C_2^*	Solubility of fraction 2, kg/m^3
D_z	Axial dispersion coeff., m^2/s
k_g	Fluid-side mass-transfer coeff., m/s
L	Fiber length, m
m	Total mass, kg

m_f	Lanoline mass on fiber, kg
N_f	Total number of fibers, -
P	Pressure, bar
P_n, P_m	Polynomials of x
R	Final radius, m
r	Fiber radius at time t and position z, m
R*	Change radius, m
r_0	Initial radius, m
R_B	Bed radius, m
r_v	Volumetric extraction rate, kg/m^3/s
T	Temperature, ºC
t	Time, s
u	Velocity, m/s
u(t)	Unit step function, eq.25
V_B	Bed volume, m3
w(x)	Weighting function, eq. 27
w´	Mass flowrate, kg/h
x	Dimensionless bed length, = z/Z_t
X	Fraction extracted,
Y	Relative concentration, =C/C_1*
Y*	Relative solubility, = C^*/C_1*
Y_{12}*	Dimensionless variable, eq. 26
z	Coordinate from bed inlet, m
Z_t	Total bed length, m

Geek symbols

α	Value in u(t), eq. 25
ε	Bed porosity at time t,
ε_0	Initial bed porosity, t=0
η	Dimensionless radius, = r/R
η_0	Initial dimensionless radius, = r_0/R
θ	Solvent residence time, = Z_t/u, s
ρ_l	Lanoline density, kg/m^3
ρ_w	Wool density, kg/m^3
τ	Dimensionless time,
ξ	Volume. solubility fraction= C_1^*/ρ_l
ψ	Mass transfer ratio, = $k_g\theta/r_0$
δ_{nm}	Kronecker´s delta,

Acronyms

OC	Orthogonal collocation
SCF	Supercritical fluid
SCM	Shrinking-core model

References

[1] Thewlis J., Lanoline for cosmetic applications, Agro food industry hi-tech, may-june vol. (1977) 14-20

[2] Whalley, G.R., Take a closer look at lanoline, TAPPI Journal, 81(5)(1998), 11-18.

[3] F.W. Jones, D.R. Bateup, S.R.Dixon, S.R. Gray SR, Solubility of wool wax in supercritical carbon dioxide, J. Supercrit. Fluids, 10 (1995) 100-111.

[4] M. Cygnarowicz-Provost, J. W. King, W. N. Marmer, P. Magidman, Extraction of woolgrease with supercritical carbon dioxide, J. Am. Oil Chem. Soc., 71 (1994) 222–225.

[5] B.S. Kuo, J.C. Kim, J.H. Jeon, H.K. Bae, Desorption of wool grease from greasy wool with supercritical carbon dioxide, Hwahak Konghak, 30 (1992) 491-498

[6] V. Eychenne, S. Sáiz, F. Trabelsi, F. Recasens, Near-critical solvent extraction of wool with modified carbon dioxide—experimental results, J. Supercrit. fluids, 21 (2001), 23-31

[7] J.M. Bayona, P. Erra, Z. Moldovan, C. Domínguez, E. Jover, F.Recasens, M.A. Larrayoz, Method for obtaining lipid fractions from wool or lanoline using pressurized carbon dioxide, Patent WO 2002100990A1, Oficina Española de Patentes y Marcas, Madrid, filed 16.07.2005

[8] C.Domínguez, E. Jover, F. Garde, J.M. Bayona, P. Erra, Characterization of supercritical fluid extracts from raw wool by TLC-FID and GC-MS, J. Am. Chem. Oil Soc., 80 (2003) 717-724.

[9] C. Domínguez, P. Erra, J.M. Bayona, Physico-chemical and dyieng properties of raw wool extracted by pressurized CO2/Modifiers, Textile research, 80 (2010) 651-659

[10] M. López-Mesas, F. Carrillo, M.C. Gutiérrez, M. Crespi, Alternative methods for wool wax extraction from wool scouring wastes, Aceites y grasas, 58 (2007) 402-407

[11] A. Valverde, PhD Thesis, in preparation, 2018

[12] P. R. Fields, T. L. Chester, A. M. Stalcup,Viscosity estimation in binary and ternary supercritical fluid mixtures containing carbon dioxide using a supercritical fluid chromatograph, J. Liquid Chrom. & Rel. Technol., 34 (2011), 995-1003

[13] M. Fullana, F. Trabelsi, F. Recasens, Use of neural net computing for statistical and kinetic modelling and simulation of supercritical fluid extractors, Chem. Eng. Sci., 54 (1999) , 5845-5862

[14] J. V. Villadsen, W. E. Stewart, Solution of boundary-value problems by orthogonal collocation, Chem. Eng. Sci., 22 (1967), 1483–1501

[15] B.A. Finlayson, Packed bed reactor analysis by orthogonal collocation, Chem. Eng. Sci., 26 (1971) 1081-1091

[16] M. Morbidelli, A. Servida, G. Storti, R. Paludetto, S. Carrà, Application of the orthogonal collocation method to some chemical engineering problems, Eng. Chim. Ital. 19 (1983) 47-60

[17] A. S. Olagunju, L. J. Folake, M. T. Raji, Comparative study of the effect of different collocation points on Legendre-collocation methods of solving second-order boundary value problems, IOSR J. Mathematics, 7 (2013) 35-41

[18] M. R. Spiegel, Advanced mathematics for engineers and scientists, McGraw-Hill, New York, 1971

[19] A. Valverde, L. Osmieri, F. Recasens, Binary interaction parameters from reacting mixture data. Supercritical biodiesel process with CO_2 as cosolvent, J. Supercrit. Fluids, 143 (2019) 107-119

[20] G. Brunner, Gas Extraction, Steinkopff Darmstadt, Springer New York, 1994

[21] J.Puiggené, M.A. Larrayoz, F.Recasens, Free liquid-to-supercritical fluid mass transfer in packed beds, Chem. Eng. Sci., 52 (1997) 195-212

[22] C.-S. Tan, S.-K Liang, D.-C. Liou, Fluid-solid mass transfer in a supercritical fluid extractor, Chem. Eng. J., 38 (1980) 17-23

[24] H. Scott Fogler, Elements of chemical reaction engineering, fourth ed., Prentice-Hall, New York, 2006